Supplementary information (SI)

Summary: Supplementary figures in the manuscript illustrate control experiments and detailed methodological validations. SI Figure 1 documents body measurements and behavioral controls for the ErasmusLadder task. SI Figure 2 provides detailed analysis of climbing fiber patterns and validates AAV delivery methods. SI Figure 3 presents supporting data for the multi-fiber photometry calcium recordings, including setup verification and example traces.

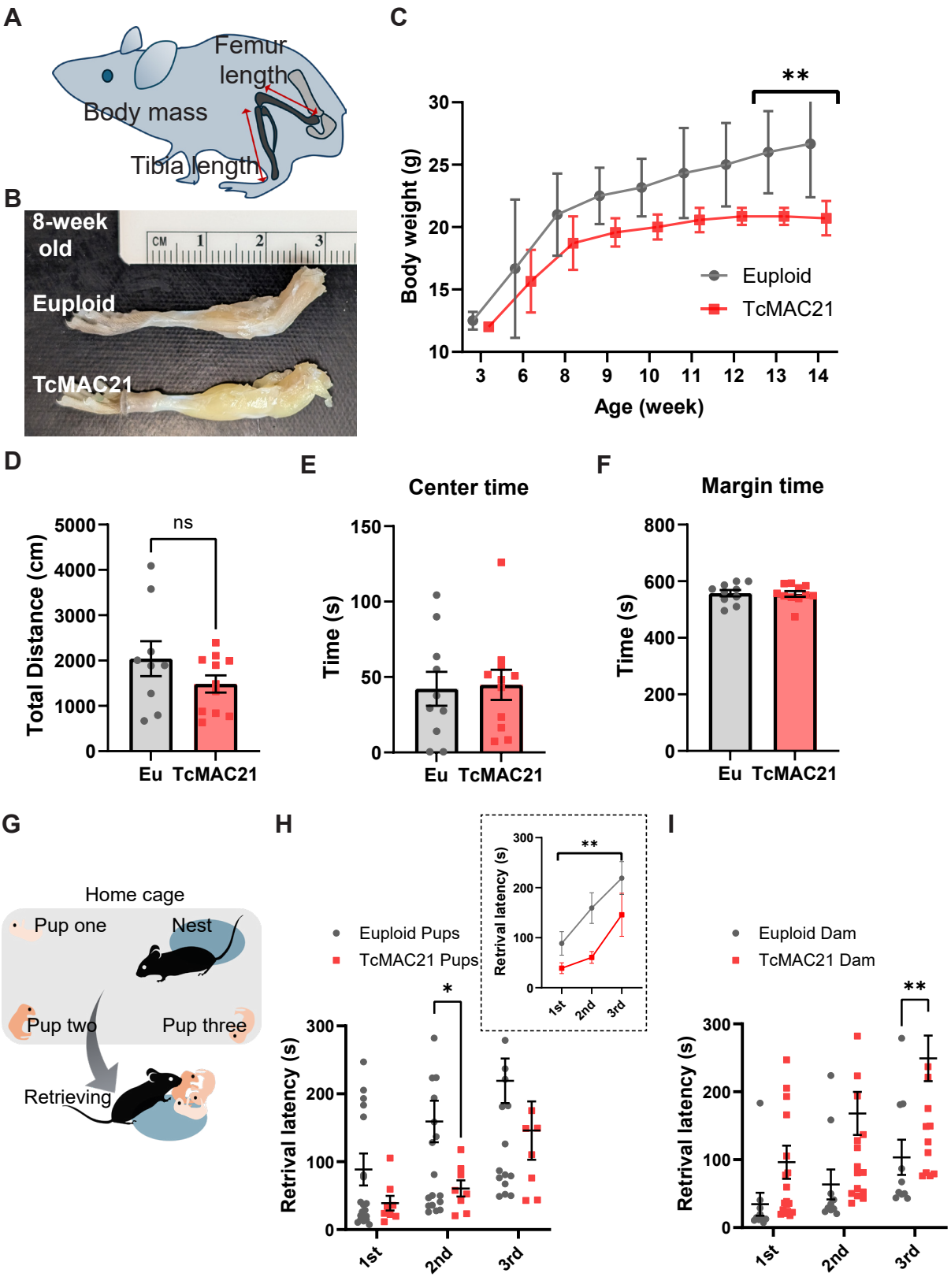

Supplementary Figure 1

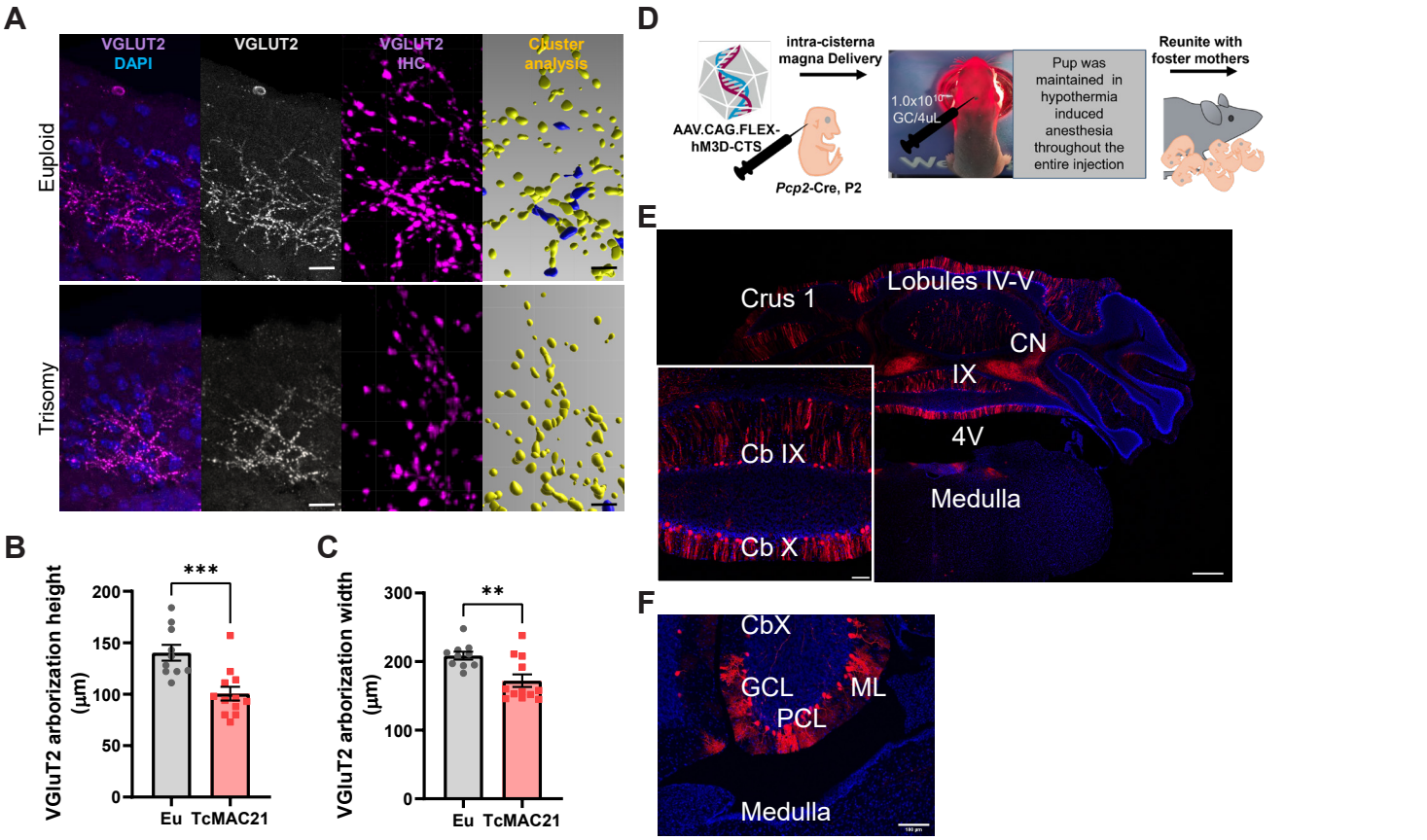

Supplementary Figure 2

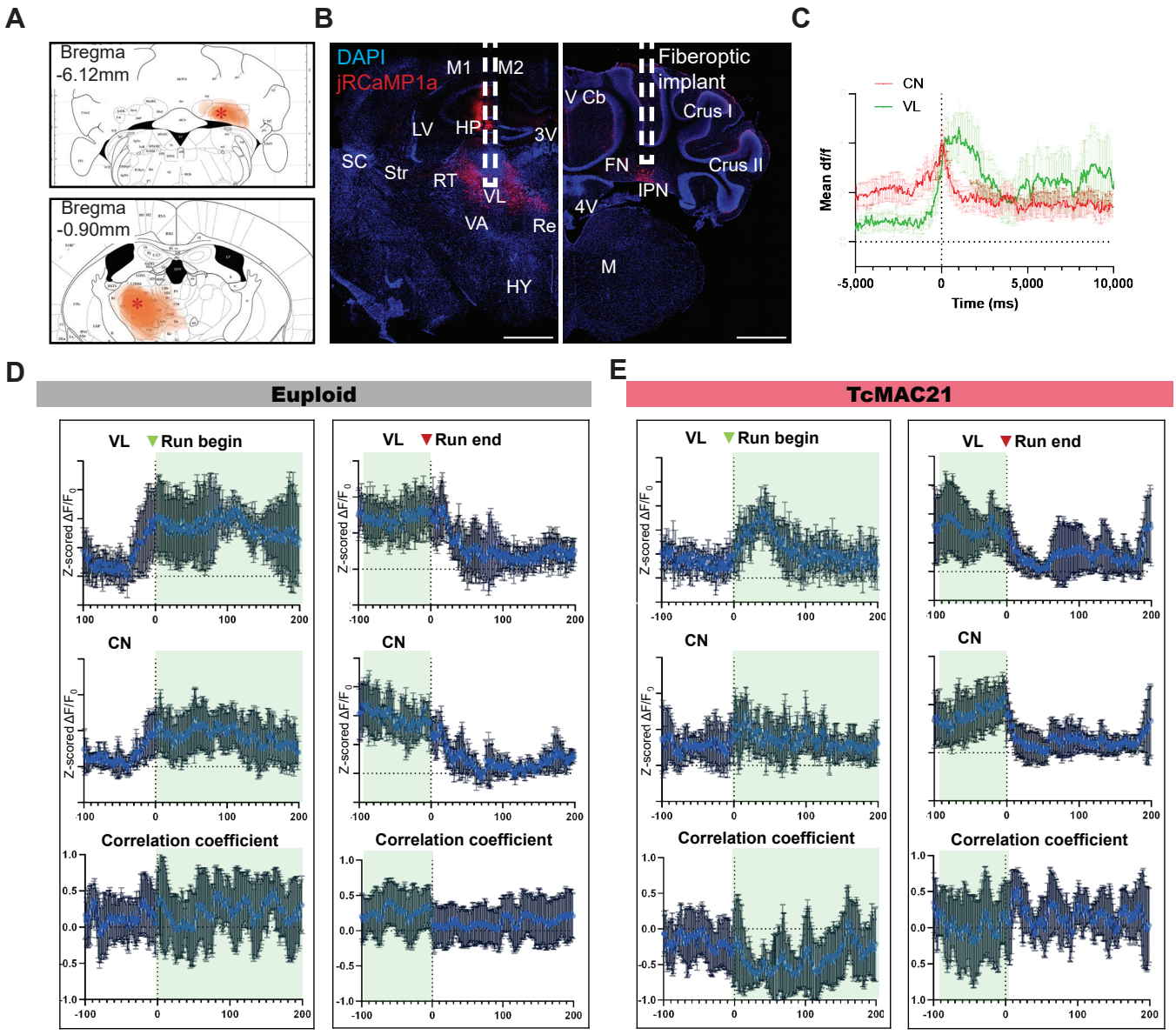

Supplementary Figure 3

Supplementary Figure 1: Body Size Measurements and Behavioral Control Experiment on Trisomic and Euploid Mice for Erasmus Ladder Motor Performance Assay, Related to Figure 1

(A and C) Femur, tibia bones, and body mass of euploid and TcMAC21 mice at 8-week-old. The schematic depiction of limb skeletal measurements in adult TcMAC21 and euploid littermates showing no significant differences in femur length (Eu: 13.87 ± 0.37 mm, TcMAC21: 13.57 ± 0.65 mm) or tibia length (Eu: 18.07 ± 0.42 mm, TcMAC21: 18.04 ± 0.69 mm). Differences were Not Significant by t-test: p = 0.7688 (C)

(B) Body weight tracked over time shows reduced weight gain in TcMAC21 mice compared to euploid controls. Data are represented as means ± SEM. Weight differences were Not Significant by unpaired t-test: p>0.9999, p>0.9999, p>0.9999, p=0.1031, p=0.0643, p=0.1994, and p=0.0735 respectively for 3-week to 12-week-old. At 13-week and 14-week-old comparisons, weight differences were Significant: *p = 0.0167 and *p = 0.0446 respectively.

(D) Evaluation of open field behavior and locomotion in neurologically intact TcMAC21 and euploid littermates at 8-week-old. Average total distance travelled in the open field revealed no significant differences in general locomotor activity or exploratory behavior, indicating that motor performance deficits in the ErasmusLadder task are not due to differences in baseline activity levels or motivation. Data are represented as means ± SEM. p = 0.2175; n = 9 for euploid mice, n = 11 for TcMAC21 mice, t-test.

(E and F) Percentage of time spent in different zones of the open field arena shows comparable exploration patterns between genotypes, suggesting no anxiety-related behavioral differences that could confound motor learning assessments. Data are represented as means ± SEM. p = 0.8634, p = 0.5532, respectively; t-test.

(G and H) Schematic presentation of Pup retrieval test. Time spent retrieving Euploid vs. TcMAC21 pups into the nest was reported. All dams were euploid. The individual pups were graphed. The inset figure depicts the summarized trend, showing retrieval latency decreased in trisomy pups. $p(1^{st})$= 0.1299, *$p(2^{nd})$= 0.0178, $p(3^{rd})$= 0.1938. Unpaired t-tests.

(I) Maternal behavior is impaired in TcMAC21 dams. The retrieval latencies of three pups on the of naive euploid and TcMAC21 dams are shown. There were significant differences between euploid and TcMAC21 dams in the retrieval latency of the third pup. Data are represented as means±SEM. $p(1^{st})$= 0.4284, *$p(2^{nd})$= 0.0639, $p(3^{rd})$= 0.0049. Unpaired t-tests.

Supplementary Figure 2: Analysis of Climbing Fiber Innervation Patterns, Related to Figure 2, and Validation of Systemic AAV Delivery for Purkinje Cell Targeting, Related to Figure 3

(A) Left: Representative sagittal cerebellar sections showing VGluT2-positive climbing fiber terminals (magenta) in the molecular layer of euploid and TcMAC21 cerebella. Right: High-res histology stack of presynaptic marker and 3D rendering of pre-synapse areas (Blue, excluded puncta; Yellow, assigned puncta). Scale bar: 50 µm and 5 µm, respectively.

(B and C) Quantification of VGluT2-positive climbing fiber extension in the molecular layer was reduced in TcMAC21 mice, measured as the molecular layer height reached by VGluT2-positive terminals. (C) Analysis of VGluT2 puncta along the dendritic arbors of Purkinje neurons. Analysis showed Significant decreased in both height and width. Data are represented as means ± SEM. ***p = 0.0009, **p = 0.5532, respectively; n = 9 for euploid cerebella, n = 11 for TcMAC21 cerebella, t-test.

(D) Schematics of the surgical approaches for Intra-Cisterna Magna (ICM) injection cre-dependent DREADD AAV virus for restricted Purkinje neurons expression during postnatal period.
(E) Representative images showing widespread viral transduction following systematic delivery of AAV.CAG.FLEX-hM3D-CTS (1x10^10 VG per animal, labelled by co-expression of RFP in Red) via ICM delivery at P2. Scale bar: 500 μm.
(F) Higher magnification images showing specific expression in Purkinje neurons with complete cell morphology labeling including dendrites and axons. Quantification of viral targeting specificity showing 66.87 ± 3.36 % of Calbindin-positive Purkinje neurons co-expressed RFP in lobule X. Scale bar: 100 μm.

Supplementary Figure 3: Supporting Data for Multi-Fiber Photometry Calcium Recordings, Related to Figure 5
(A) Schematic of a mouse brain coronal section showing jRCaMP1a reporter expression from cerebellar nuclei (CN) and ventrolateral thalamus (VL). Asterisk designates sites of viral injection (CN: AP -6.13 mm, ML ±1.60 mm, DV -3.60 mm; VL: AP -0.9 mm, ML ±1.00 mm, DV -3.75 mm relative to bregma). Restricted reporter expression spread was shown as overlapping shaded area, n = 11 animals.
(B) Representative histological verification of fiber optic cannula placements. VL (left panel) and CN (right panel) targeting showing fiber tract above confined jRCaMP1a expression (red) area. DAPI counterstain in blue. Brain region abbreviations -M1: Primary Motor Cortex, M2: Secondary Motor Cortex, LV: Lateral Ventricle, HP: Hippocampus, 3V: Third Ventricle, Str: Striatum, RT: Reticular Thalamic Nucleus, VL: Ventrolateral Thalamic Nucleus, VA: Ventral Anterior Thalamic Nucleus, Re: Reuniens Thalamic Nucleus, HY: Hypothalamus, FN: Fastigial Nucleus (of the cerebellum), IPN: Interposed Nucleus (of the cerebellum), V Cb: Lobule V of the Cerebellar Vermis. Scale bars: 1000 μm.
(C) Example traces showing simultaneous calcium signals (mean ΔF/F) recorded from an euploid mouse in CN (red) and VL (green) during the transition (t=0) from stationary to running periods.
(D) Example traces from a euploid mouse showing increased synchronicity between CN and VL calcium signals during locomotor phase compared to stationary phase.
(E) Example traces from a TcMAC21 mouse showing decreased temporal synchronicity during running phase compared to euploid.